

## Simultaneous Detection of Multifood-Borne Pathogenic Bacteria Based on Functionalized Quantum Dots Coupled with Immunomagnetic Separation in Food Samples

YU ZHAO,<sup>†</sup> MINGQIANG YE,<sup>†</sup> QIANGGUO CHAO,<sup>‡</sup> NENGQIN JIA,<sup>†</sup> YU GE,<sup>‡</sup> AND  
 HEBAI SHEN<sup>\*·†</sup>

Department of Chemistry, Life and Environment Science College, Shanghai Normal University, 100 Guilin Road, Shanghai 200234, People's Republic of China, and Shanghai Institute of Quality Inspection and Technical Research, 381 Cangwu Road, Shanghai 200233, People's Republic of China

This paper reports a method that simultaneously detects three food-borne pathogenic bacteria, *Salmonella typhimurium*, *Shigella flexneri*, and *Escherichia coli* O157:H7, via an approach that combines magnetic microparticles for the enrichment and antibody-conjugated semiconductor quantum dots (QDs) as fluorescence markers. Using the water-in-oil reverse microemulsions method, the  $\gamma$ -Fe<sub>2</sub>O<sub>3</sub> magnetic nanoparticles were coated with silica to empower the particles with high dispersibility and broad compatibility to biomacromolecules. The magnetic beads were then modified with amino silane, which could immobilize antibodies by glutaraldehyde treatment. The immunized magnetic beads and pathogenic bacteria formed "bead-cell" complexes in the enrichment procedure. QDs with different emission wavelengths (620, 560, and 520 nm) were immobilized with anti-*S. typhimurium* antibody, anti-*S. flexneri* antibody, and anti-*E. coli* O157:H7 antibody, respectively. Fluorescence microscope images and the fluorescence intensity of QDs labeled "sandwich" complexes (conjugated with antibodies against *S. typhimurium*, *S. flexneri*, and *E. coli* O157:H7, respectively) demonstrated that antibody-conjugated QDs could attach to the surface of bacterial cells selectively and specifically. In our method, we could detect food-borne pathogen bacteria in a food matrix at 10<sup>-3</sup> cfu/mL. We determined that a high concentration of proteins in food matrix would decrease the sensitivity of this method. This method, of which the detection procedures are completed within 2 h, can be applied to the rapid and cost-effective monitoring of bacterial contamination in food samples.

**KEYWORDS:** Immunoassay; nanoparticles; quantum dot; food borne; fluorescence

### INTRODUCTION

Food-borne pathogenic bacteria are a broad spectrum of microbial pathogens and are widely responsible for many food-borne diseases. In the United States, food-borne pathogens may be responsible for as many as 76 million cases of illness each year, among over 300 000 hospitalizations, and over 5000 deaths (*1*). A report presented by a national food-borne disease surveillance system of China showed that between 1994 and 2003, 37% of food-borne disease events and 52% of food-borne disease cases were caused by microbial pathogens. Among these cases and events, 22, 6, and 2% were attributable to *Salmonella*, *Escherichia coli*, and *Shigella* infections, respectively (*2*). In addition, *Salmonella typhimurium*, *Escherichia coli* O157:H7, and *Shigella flexneri* are three of the most important strains

spreading throughout various food items. Because of the low infectious dose and high health risk of food-borne pathogens, there is an urgent need for the development of rapid, sensitive, and reliable approaches to stringently monitor different food-borne pathogens. In recent years, several methods have been developed on this issue based on molecular and immunological theory. Multiplex polymerase chain reaction (PCR) is an important method, which can detect as many as eight food-borne pathogenic bacteria in one assay (*3*). DNA microarray is another method for the detection and characterization of multiple food-borne pathogens based upon the hybridization of oligonucleotide probes (*4*). Immunochemical methods including enzyme-linked immunosorbent assays (ELISAs) (*5*), immunomagnetic separation (IMS) methods (*6, 7*), and fluorescence-based assays using organic dye molecules (*8*) usually involve fluorophore-labeled antibodies with different specificities for different antigens present in the samples. *E. coli* O157:H7 (*9*), *Salmonella* (*10*), *Shigella* (*11*), and many other bacterial pathogens have been successfully detected based on the methods

\* To whom correspondence should be addressed. Tel: (86)21-64321800. Fax: (86)21-54242640. E-mail: shenhb@shnu.edu.cn.

<sup>†</sup> Shanghai Normal University.

<sup>‡</sup> Shanghai Institute of Quality Inspection and Technical Research.

using fluorophores such as fluorescein isothiocyanate (FITC). However, there are significant limitations of traditional dyes in multicolor immunoassays, such as rapid photobleaching, a narrow excitation spectrum, and low signal intensities. Recent advances in nanotechnology have provided a novel and promising class of fluorescent labels due to their optical and electronic advantages over conventional fluorophores (12). It is estimated that CdTe quantum dots (QDs) are by about 2 orders brighter and by 3 orders more stable against photobleaching than ordinary dyes (12). More importantly, QDs can be excited efficiently at any wavelength shorter than the emission peak yet will emit the same narrow, symmetric characteristic spectrum regardless of the excitation wavelength. This unique property makes it possible to detect different emission peaks simultaneously when different sizes of QDs are excited with a single wavelength. QDs have been used as fluorescent labels for the multicolor imaging of tissues (13) and the detection of toxins (14). The use of QDs has also been extended to multicolor detection based on immunoassay formats for microorganism detection (7, 15). A fluorescence system, utilizing QDs as fluorescent labels, has been developed and has exhibited superior photostability than traditional organic dyes in detection and has allowed dual color for *Cryptosporidium parvum* and *Giardia lamblia* (16). It has been proven that two food-borne strains, *E. coli* O157:H7 and *S. typhimurium*, labeled with bifunctionalized QDs, were identified simultaneously (17).

In this paper, we report a novel protocol for simultaneous detection of three food-borne bacterial strains with biolabeling QDs coupled with IMS in the same assay. QDs with different emission wavelengths were conjugated to antibodies of three major food-borne bacterial strains (*S. typhimurium*, *E. coli* O157:H7, and *S. flexneri*, respectively). Moreover, target bacteria were separated from samples by using specific antibodies coated with magnetic beads. The "bead-cell" complexes reacted with QD-antibody conjugates to form "sandwich" complexes. The intensities of the different emission peaks illustrated the determination and quantification of target strains.

## MATERIALS AND METHODS

**Reagents.** CdTe QDs (emission, 620, 560, and 520 nm; diameter, 2–5 nm) were kindly provided by the Institute of Chemistry, Chinese Academy of Sciences. Rabbit anti-*Salmonella* antibody (2–3 mg/mL) and anti-*S. flexneri* antibody (2–3 mg/mL) were purchased from Lanzhou Institute of Biological Products (China). Biotechnology Inc. Rabbit anti-*E. coli* O157:H7 antibody (2–3 mg/mL) was purchased from Ningbo Scientz Biotechnology Co. Limited (China). Biotechnology Inc. 1-(3-dimethylaminopropyl)-3-ethylcarbodiimide hydrochloride (EDAC) and N-hydroxysulfosuccinimide sodium salt (NHSS) were purchased from Acros-Organics. Nutrient broth medium (NB), bismuth sulfite agar (BS), sorbitol Maconkey agar (SM), and *Salmonella Shigella* agar (SS) were supplied by Beijing Land Bridge Technology Co. Limited. Common solvents and salts were supplied by Xinghua Chemical Plant of Shanghai (Shanghai, People's Republic of China).

**Synthesis and Immunization of Superparamagnetic Nanoparticles.** The synthesis of silica-coated superparamagnetic nanoparticles was prepared by our reported method (18). Typically, a 2.5 M NaOH solution was dropped into the solution of a mixture of FeCl<sub>3</sub> (0.2 M) and FeSO<sub>4</sub> (0.12 M) with violent stirring. The obtained precipitation was aged and washed with water and dried and translated into a magnetic core ( $\gamma$ -Fe<sub>2</sub>O<sub>3</sub>). To coat the magnetic nanoparticles with silica, a water-in-oil reverse microemulsion of water/Triton X-100/*n*-hexylalcohol/cyclohexane was adopted. In this reaction, 0.1 g of  $\gamma$ -Fe<sub>2</sub>O<sub>3</sub> was dispersed in the 60 mL above the microemulsion with ultrasonication. Next, concentrated ammonia and tetraethoxysilane (TEOS) were added dropwise into the system in turn. The reaction was ended after 10 h, and the nanoparticles were aged overnight. Thereafter, the mixture was washed with ethanol three times and calcined to demineralize useless

**Table 1.** Results of the Fluorescence Signal Obtained from the Different Concentrations of Cross-Linker and Protective Solution in Mixture<sup>a</sup>

cross-linker		protective solution	
EDAC (final) (mg/mL)	signal	NHSS (final) (mg/mL)	signal
0	+++	0	+++
10	+++	2	+++
20	+++	5	+++
30	++	10	++
40	+	15	+
50	–	20	–

<sup>a</sup> Shows the intensity of the fluorescent signal under fluorescence microscopy, as compared with that emitted by no EDAC solution.

organic compound. N-[3-(Trimethoxysilyl)propyl]ethylene diamine (AEAPS) was chosen to modify these superparamagnetic nanoparticles for its further use in the organism. Twenty milligrams of nanoparticles was dispersed in a mixture of 25 mL of methanol and 15 mL of glycerol with ultrasonication. One and a half milliliters of AEAPS was added into the mixture and dispersed by vigorous stirring. Finally, the amino-silane-modified nanoparticles were washed with methanol several times and kept in double-distilled water.

The amino-silane-modified silica-coated  $\gamma$ -Fe<sub>2</sub>O<sub>3</sub> was used to immobilize the antibody. According to a previous report, glutaraldehyde was adopted to activate the nanoparticles; other conditions of the immobilization have not been discussed here, and the optimal conditions were taken, as other literature has reported (19). Specially, 0.1 mL (10  $\mu$ g) of amino-silane-modified nanoparticles was poured into 1 mL (mass fraction = 2.5%) of glutaraldehyde solution at room temperature. After 4 h of reaction, magnetic nanoparticles of hydroformylation were reserved under certain magnetic fields, and unreacted glutaraldehyde was poured out. Thereafter, 40  $\mu$ L (2 mg/mL) of anti-*E. coli* O157:H7 antibodies was added into the above system and kept at room temperature for 2 h. Finally, magnetic nanoparticles of immunization were reserved and washed in the presence of an exterior magnet. These products were collected and kept at 0–4 °C. In accordance with the same methods, anti-*S. typhimurium* antibodies and anti-*S. flexneri* antibodies, respectively, were reacted with functionalized nanoparticles activated by a 2.5% glutaraldehyde solution.

To further evaluate the protein immobilization capacity of the functional magnetic nanoparticles, bovine serum albumin (BSA), a specific protein extracted from bovine serum, was taken as a control sample. A series of known concentrations of BSA were measured with Cary100 ultraviolet spectrophotometer to get the OD<sub>280</sub> values, and a standard curve could be obtained from known concentrations and OD<sub>280</sub> values of BSA. Sixty microliters of BSA of unknown concentration was poured into a 1 mL system with 10  $\mu$ g of functional nanoparticles activated by a 2.5% glutaraldehyde solution, and then, the mixed solutions were left at room temperature with continuous shaking for 2 h. The proteins immobilized by the magnetic nanoparticles were obtained using magnetic separators. The amount of the proteins immobilized by the magnetic nanoparticles was determined by measuring the absorption at 280 nm of the initial and the final supernatant.

**Covalent Immobilization of the Antibody onto Functionalized QDs.** Carboxylate-modified highly luminescent semiconductor CdTe QDs (emission, 620, 560, and 520 nm; diameter, 2–5 nm) were conjugated to anti-*S. typhimurium* antibodies, anti-*S. flexneri* antibodies, and anti-*E. coli* O157:H7 antibodies using the solution of EDAC/sulfonamide compounds as "coupling reagents" (20, 21). Different concentrations of chemical reagents were used to carry out a series of experiments; the stability of the fluorescence signal and the joint efficiency of conjugates between QDs and antibody were thus studied in **Table 1**. Furthermore, to make good use of QDs and good conjugation, QDs and antibody had a mole ratio between 1:10 and 1:40 (22). Particularly, 20  $\mu$ L (about  $2.6 \times 10^{-6}$  mol) of QDs stock solution was added to the mixed solution containing 40  $\mu$ L of axenic phosphate-buffered solution (PBS, 0.01 mol/L, pH 7.2) and 2 mg (final, 20 mg/mL) of EDAC. Next, the mixture was vortexed for 5 min at room temperature and took about 15–20 min to fully activate free carboxylic

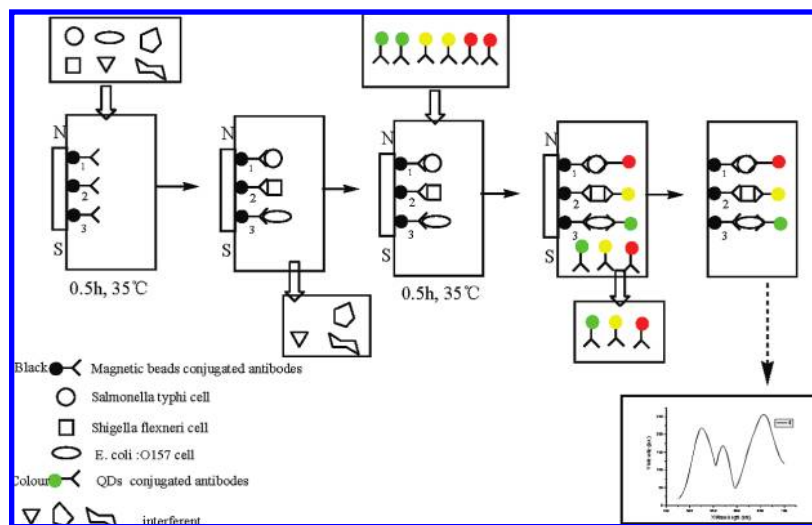


**Figure 1.** Schematic illustration of the entire immunoassay procedure for detecting three pathogenic strains. The immunomagnetic beads were first immobilized on the well of the separator by a magnet. The sample matrix containing three strains (*S. typhimurium*, *S. flexneri*, and *E. coli* O157:H7, respectively) was specifically enriched and separated from the mixture. QD-antibody conjugates were used as fluorescence labels through the immunorecognition between antibodies and target cells.

acid groups on the QDs. Similarly, 0.5 mg (final, 5 mg/mL) of Sulfo-NHS was put into the upper mixed solution and vortexed for 15 min at room temperature. In this step, semistable amine-reactive NHS-ester could be synthesized by the esterification of the activated carboxylic acid groups on the QDs and hydroxyl groups on the Sulfo-NHS. Thereafter, 40  $\mu\text{L}$  of antibodies was added into the system and was vortexed for at least 2 h. Finally, unreacted antibody molecules were removed from the media by centrifugal concentrators (Vivaspin 500 centrifugal concentrators, 300 KD). QDs and antibodies were connected through strong covalent bonds. The final products were collected and kept at 0–4  $^{\circ}\text{C}$ .

An electrophoresis apparatus (Bio-Rad, PowerPac Basic) was applied to characterize the efficiency of the combination between QDs and antibodies (23). A 6% polyacrylamide separating gel was run at 15 V/cm with a running buffer composed of 24.8 mM Tris, 0.189 M glycine, and 0.1% (w/v) sodium dodecyl sulfate (SDS). After electrophoresis, the gel was stained for about 1 h in a mixture containing 0.1% (w/v) Coomassie brilliant blue R-250, 50% methanol, and 10% glacial acetic acid and then destained in the same solution without Coomassie brilliant blue R-250.

A fluorophotometer was used to measure the fluorescence intensity (FI) of three kinds of QDs-Ab conjugates and QDs. In accordance with the above-described connection method of using the solution of EDAC/sulfo-NHS compounds as “coupling reagents”, the concentration of QDs was about  $2.17 \times 10^{-7}$  mol/L, and the ratio of QDs:antibody:EDAC:NHSS by mole was about 1:10:20:5 in the reaction. Three kinds of 600  $\mu\text{L}$  of QDs-Ab conjugates were, respectively, put into the standard 10 mm cell and measured with a Hitachi F-2500 fluorophotometer with 150 W xenon lamp. At the same time, three kinds of 600  $\mu\text{L}$  of QDs with the same concentration mentioned above were, respectively, measured with the same machine and parameter.

**Bacterial Inocula Preparation and Agar Plate Count.** Stock cultures of *S. typhimurium* (ATCC 50013), *E. coli* O157:H7 (ATCC 25922), and *S. flexneri* (ATCC 51573) were obtained from Shanghai Institute of Quality Inspection and Technical Research (SQI). Cultures were grown for 15–18 h at 37  $^{\circ}\text{C}$  in ordinary NB. Serial 10-fold dilutions were made in axenic PBS (0.01 mol/L, pH 7.2). The number of *S. typhimurium*, *E. coli* O157:H7, and *S. flexneri* was determined by surface plating technology using 0.1 mL proper dilutions onto BS, SM, and SS, respectively. After incubation at 37  $^{\circ}\text{C}$  for 24–48 h (BS = 48 h and SS and SM = 24 h), colonies on the plates were counted to determine the number of viable bacteria in the dilutions in terms of colony units per milliliter (cfu/mL). For safety considerations, all of the bacterial samples were placed in an autoclave at 100  $^{\circ}\text{C}$  for 20 min to kill bacteria, except for some special tests and characterizations.

**Immunologic Process.** The basic principles of enrichment and immunoassay procedures for detection of the three species of food-borne bacteria are shown in **Figure 1**. In this schematic, *S. typhimurium*, *E. coli* O157:H7, and *S. flexneri* were first captured by immunomagnetic beads (conjugated with anti-*S. typhimurium* antibodies, anti-*E. coli* O157:H7 antibodies, and anti-*S. flexneri* antibodies, respectively). In this procedure, 90  $\mu\text{L}$  of mixed antibody immobilized magnetic beads (containing each type of immunomagnetic beads) was moved into a microcentrifuge tube fastened on a magnetic separator, and 3 mL of bacterial samples (containing different dilutions of *S. typhimurium*, *E. coli* O157:H7, and *S. flexneri*, respectively) was moved into the tube and kept at room temperature for 0.5 h. Next, the leftover liquid of the whole system was poured out. The “bead-cell” complex was separated using a magnetic separator. The mixture was washed with PBS (pH 7.4) three times. Secondary, antibody-immobilized QDs were added into the above “bead-cell” complex to form “bead-cell-QDs” conjugates. To perform this step, 50  $\mu\text{L}$  of mixed antibody-immobilized QDs was put into the tube and kept at room temperature for 0.5 h. After reaction, these mixtures were washed three times with PBS and separated from the solution using magnetic separators again. The mixture was suspended with 600  $\mu\text{L}$  of PBS.

For the stability of the QDs, it was possible to carry out quantitative analysis of detecting bacterial pathogens in this experiment. In this procedure, 3 mL of five dilution levels for each microorganism ( $10^5$ ,  $10^4$ ,  $10^3$ ,  $10^2$ , and 10 cfu/mL, respectively) was chosen as a test sample. Three milliliters of distilled water was treated, using the same procedure, as a control. The leftover liquid was poured out, and the “bead-cell” complexes were washed with PBS three times and were diluted with 200  $\mu\text{L}$  of PBS. Second, 50  $\mu\text{L}$  of mixed antibody-immobilized QDs was put into these tubes and kept at room temperature for 0.5 h. Next, these mixtures were washed three times with PBS using magnetic separators again and were suspended with 600  $\mu\text{L}$  of PBS. It was very important to keep the magnetic separator motionless throughout the whole process of the experiment. By means of keeping the magnetic separator motionless throughout the whole process of the experiment, antigen binding sites of pathogens were left to antibody immobilize QDs, and it was very important to improve the sensitivity of this assay. The key step of the whole experiment was the first step shown in **Figure 1**. Finally, these “sandwich” complexes’s fluorescence images were captured from fluorescence microscopy and their FIs were measured with a fluorophotometer.

**Fluorescence Microscopic Photos and Deconvolution of Composite Spectra.** A fluorescence microscope (Olympus, BX51), equipped with a digital CCD camera (Olympus DP70) and a broadband mercury lamp (OSRAM HBO 100W) with an ultraviolet excitation filter, was also used to capture images of “sandwich” complexes, which were

dropped onto the glass slides. The “sandwich” complexes were subjected to fluorescence measurement with an instrumentation system consisting of a fluorophotometer (Hitachi F-2500) with a 150 W xenon lamp. To investigate the FI of the “sandwich” complex, 600  $\mu\text{L}$  of the complex was put into the standard 10 mm cell. Other items set for scan were as follows: excitation, 270 nm; emission, from 450 to 700 nm; slit width, 5 nm; wavelength scan speed, 300 nm  $\text{min}^{-1}$ ; and voltage, 700 V. The narrow and symmetric emission profile of QDs allowed simple deconvolution of the composite signal to generate individual QD photoluminescence (PL) contributions (24, 25). Several QD-antibody bioconjugates, each having a unique PL spectrum functioning as independent signal channels, were used to assess the feasibility of a QD-based multiplexing system. The resulting composite spectra were deconvoluted using the known QD emission profiles to reveal individual contributions of each QD population.

**Sample Preparation.** The protocols developed were used to determine the presence of *S. typhimurium*, *E. coli* O157:H7, and *S. flexneri* in apple juice and milk collected from local producers in the Shanghai region (Eastern area of China). Three bacterial strains (*S. typhimurium*, *E. coli* O157:H7, and *S. flexneri*) and one control strain (*E. coli* DH5 $\alpha$ ) were cultured in a flask with 100 mL of NB medium at 37 °C and shaken at 100 rpm. To reach a concentration of  $10^9$  cfu/mL, these flasks were cultured overnight.

The dilution series of the original samples was generated using autoclaved apple juice and pasteurized milk  $\times 10^8$ ,  $10^7$ ,  $10^6$ ,  $10^5$ ,  $10^4$ ,  $10^3$ ,  $10^2$ , and 10, to obtain microorganism-in-food samples at five different concentration levels for each microorganism ( $10^6$ ,  $10^5$ ,  $10^4$ , and  $10^3$  cfu/mL, respectively). One sample containing mixed culture broth (20 mL of *S. typhimurium*, *E. coli* O157:H7, and *S. flexneri*, at a dilution of  $10^6$ ) was named mixed sample (MS). To investigate the influence of protein and lipids in this method, the milk sample was diluted 10-fold by sterile physiological saline first. The single strains and mixture of the three strains were then diluted by these milk samples to generate cell concentrations at  $\sim 10^5$ . One dilution series not containing test microorganism was selected as the background. According to protocol of China national standard of microbiological examination of food hygienic determination, 25 mL of these food samples (single species, mixed culture, and negative control, respectively) was diluted in 225 mL of sterile physiological saline solution. All of the concentrations were used for IMS-antibody-QDs analysis. These food samples also detected *S. typhimurium*, *E. coli* O157:H7, and *S. flexneri* according to China national standard of microbiological examination of food hygienic determination (GB/T 4789.4-2003, GB/T 4789.5-2003, and GB/T 4789.6-2003, respectively) as a control at the same time. In this procedure, 1 mL of sample (containing a single species, mixed culture, and negative control, respectively) from 250 mL of mixture was first cultured in 10 mL of NB at 37 °C overnight. Next, these culture were streaked on selective medium (BS for *S. typhimurium*, Chrom agar O157 for *E. coli* O157:H7, and SM for *S. flexneri*, respectively) and kept at 37 °C overnight. A specific colonial morphology of detected food-borne bacteria appeared on these agar plates.

## RESULTS AND DISCUSSION

**Synthesis and Characterization of Functionalized Magnetic Beads.** The  $\gamma\text{-Fe}_2\text{O}_3$  magnetic nanoparticles used in this experiment were synthesized by the coprecipitation method. Because they tend to aggregate into large clusters, the uncoated nanoparticles lose the specific properties and thus cannot be used directly (26). In this study, the  $\gamma\text{-Fe}_2\text{O}_3$  nanoparticles have been coated with silica to provide the particles with a high dispersibility and broad compatibility to biomacromolecules. The sample of the silica-coated magnetic nanoparticles has been dropped on a carbon-coated copper grid and dried at room temperature. A Hitachi-600 TEM has been used to study the size, distribution, and morphology of the silica-coated magnetic nanoparticles. **Figure 2** shows that the nanoparticles are ideally dispersed and that the average diameter of the nanoparticles is about 60 nm.

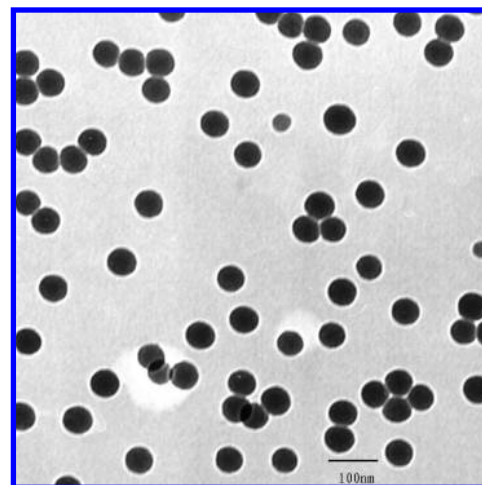


**Figure 2.** TEM micrograph of silica-coated  $\gamma\text{-Fe}_2\text{O}_3$  nanoparticles at 100 000 $\times$  magnification.

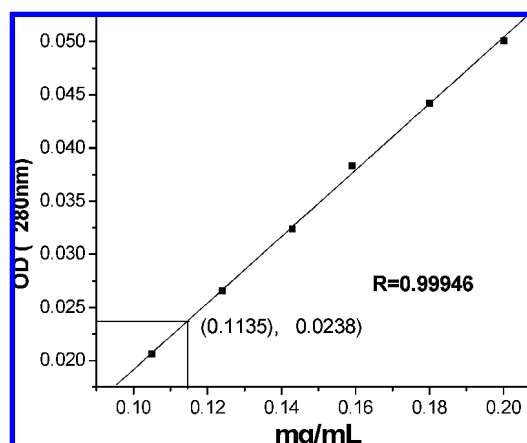


**Figure 3.** Calibration curve of bovine serum albumin (BSA) density and  $\text{OD}_{280}$ .

AEAPS was chosen to modify these superparamagnetic nanoparticles. After they were activated by glutaraldehyde, amino groups on the surface of the particles were changed into aldehyde groups, which could react with the amino groups on antibodies. In this experiment, BSA was used as the control sample. **Figure 3** shows the standard curve correlating the concentrations and the  $\text{OD}_{280}$  values of BSA in solution, and the correlation coefficient is 0.99946. The unknown concentration of BSA could thus be calculated according to the standard curve and its  $\text{OD}_{280}$  value. **Figure 4** shows the immobilization ability of the functional magnetic nanoparticles. Deducing from the standard curve and the difference  $\text{OD}_{280}$  values of the initial and the final supernatant, the calculated immobilization ability of the functional magnetic nanoparticles is about 0.1135  $\text{mg mL}^{-1}$ .

**Preparation and Characterization of Immunized QDs.** The protocol that utilizes EDAC/sulfo-NHS compounds as “coupling reagents” has been applied in this study. Because of the presence of primary amine groups, many kinds of proteins do not need any chemical modification before they can be conjugated to QDs; QDs and antibodies can be firmly linked by covalent immobilization. For stable fluorescent signals and good linkage between QDs and anti-*E. coli* O157:H7 antibodies, a series of experiments have been carried out, and the results are shown in **Table 1**. The results show that under conditions of increased concentrations of cross-linker (EDAC), the obtained fluorescence is decreased as compared

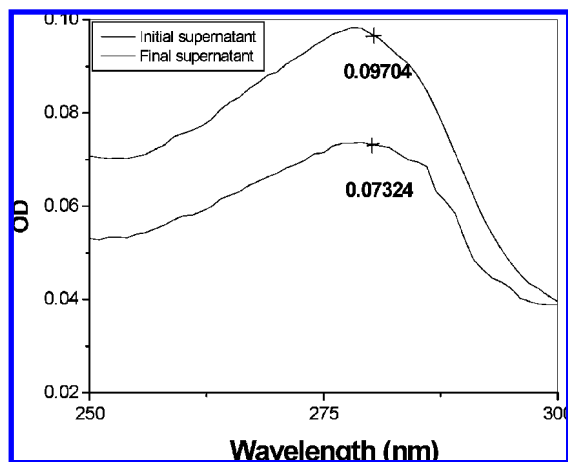


Figure 4. OD<sub>280</sub> of BSA before and after conjugation with IMS.

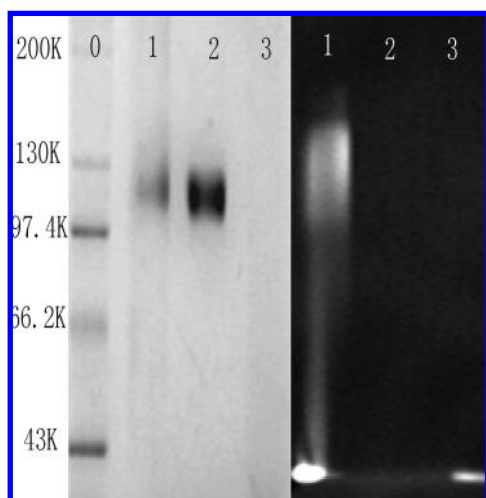


Figure 5. Six percent SDS-PAGE of a standard protein ladder (lane 0), QDs-Ab bioconjugates (lane 1), Ab (lane 2), and QDs (lane 3). The right panel is a fluorescence image, and the left panel is a bright field image obtained after staining the gel with Coomassie blue. Molecular masses marked on the left-hand side image are in kilodaltons.

to the condition where no EDAC is present. The signal is significantly decreased when the concentration of EDAC is higher than 30 mg/mL. When NHSS is used, the same situation happens when the concentration of NHSS in the mixture is increased. The reason for red-shift of the emission peak and enhancement of FI is that QDs are surrounded with organic layers (antibody). The results of these experiments show that the preferable ratio of QDs:EDAC:NHSS by mole is 1:20:5.

Electrophoresis [SDS-polyacrylamide gel electrophoresis (PAGE)] was exploited to access the effectiveness of the linkages of proteins with QDs (23). In this experiment, a standard protein ladder, QDs-anti-*E. coli* O157:H7 antibodies conjugates, anti-*E. coli* O157:H7 antibodies, and CdTe QDs were added to specimen insertion ports, named 0, 1, 2, and 3, respectively. Two types (images under UV and light) of pictures were taken from the same gel after electrophoresis to identify the effectiveness of the coupling reaction.

A comparison of an UV image with an image obtained by staining the gel with Coomassie Brilliant Blue is shown in Figure 5. Apparently, the fluorescence of QDs survived the electrophoresis, and the overlapping band stained by Coomassie Brilliant Blue in lane 1 suggests that the conjugation between QDs and antibody is successful. The same results have been obtained

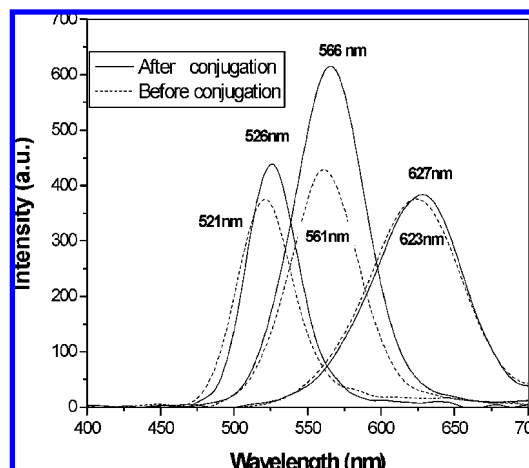
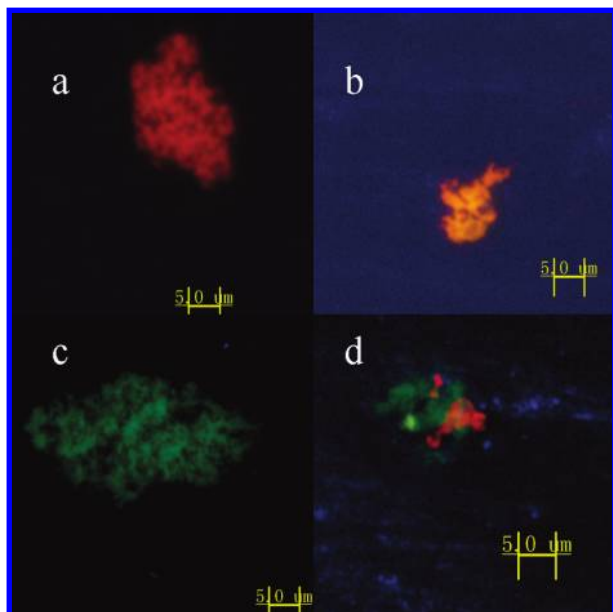


Figure 6. FI of three kinds of QDs-antibody conjugates and QDs with the same concentration.

for the conjugation of QDs with anti-*S. typhimurium* antibodies and QDs with anti-*S. flexneri* antibodies using the reported procedures (data not shown).

The FIs of three kinds of QDs-Ab conjugates and QDs have been measured and are shown in Figure 6. In Figure 6, it can be observed that the emission peak of reacted QDs had red-shifted around 4–5 nm as compared to unconjugated QDs and that the FIs of QDs-Ab conjugates had been enhanced by some counts as compared to “naked” QDs of the same concentration. The reason for the red-shift of the emission peak and the enhancement of FI is believed to be caused by the surrounding organic layer (antibody) of QDs (25).

**Fluorescence Photographs and the Deconvolution of Composite Spectra.** To investigate the selectivity and specificity of this method, three food-borne bacterial strains (*S. typhimurium*, *E. coli* O157:H7, and *S. flexneri*, respectively) have been tested under the optimized conditions. The results are shown in Figures 7 and 8. After conjugation to IMS and treatment with a magnetic separator, IMS-cell complexes will aggregate. Because of the unique properties of QDs, bacterial cells (*S. typhimurium*, *S. flexneri*, and *E. coli* O157:H7, respectively) can be visualized after they are marked with QD-antibody. Figure 7 shows the image of the final “sandwich” complex observed under a fluorescence microscope. Panels a, b, c, and d correspond to strains of *S. typhimurium*, *S. flexneri*, *E. coli* O157:H7, and the mixture of the three strains marked with QD-antibody at a dilution of  $10^5$ , respectively. In panels a, b, and c, the images of red, yellow, and green colors of QDs can be detected by a fluorescent microscope, which indicates that the QD-antibody can be conjugated to cell-IMS mixture selectively. In panel d, the image of the three different colors can be identified in a MS, which demonstrates the specificity of the conjugation between QD-antibody and cell-IMS. The FI of the final “sandwich” complexes has been measured with a fluorophotometer (Hitachi F-2500). The nearly Gaussian profiles of QDs have allowed an accurate deconvolution of fluorescence signals (24), and we have thus been able to quantitatively study the detection of multipathogenic bacteria by generating individual QD PL contributions from the simple deconvolution of the composite signals. In Figure 8, we show representative groups of fluorescence spectra obtained from different concentrations of samples containing a mixture of the three species of bacteria. As shown in the spectrum in Figure 8, the black composite spectra have been obtained from a fluorophotometer, and the three individual spectra for immunized QDs (625, 565, and 525 nm) have been deconvoluted from the composite



**Figure 7.** Fluorescent microscopic images of food-borne bacterial cells separated by magnetic beads and marked with immuno-QDs. Panels a–c show the images of single strain of *S. typhimurium*, *S. flexneri*, and *E. coli* O157:H7 in solution after treatment. Panel d shows the mixture of the three species in solution after treatment ( $10 \times 100$ ).

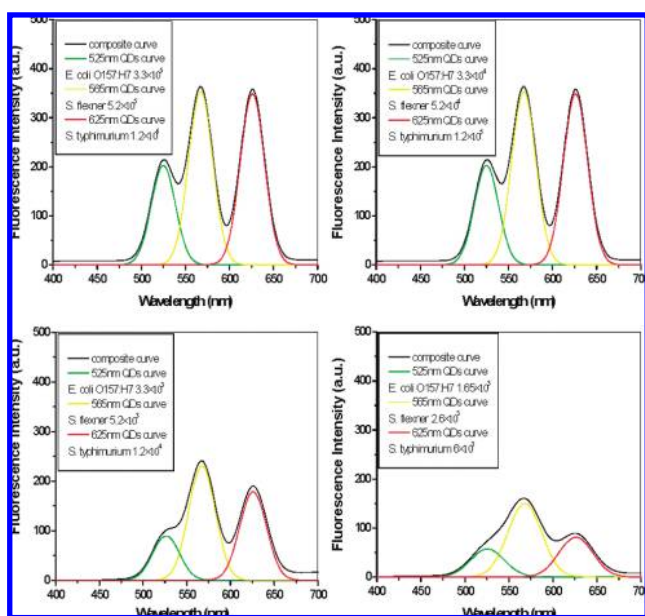


**Figure 8.** Both the composite fluorescence spectra and the deconvoluted spectra for the three individual antibody-immobilized QDs (525, 565, and 625 nm) are displayed. The composite fluorescence spectra were obtained from the samples containing different bacterial cell numbers.

spectra. The three strong peaks at 625, 565, and 525 nm represent the fluorescence signals produced by different QDs that specifically recognize *S. typhimurium*, *S. flexneri*, and *E. coli* O157:H7, respectively. This result indicates that each type of QD-antibody conjugate can bind to their target bacteria in the mixture and produce different fluorescence signals.

It can be observed in **Figure 8** that the intensity of the fluorescence peaks grows with the increasing cell numbers. While the concentration of *E. coli* O157:H7 in the mixture of the three bacteria samples increases from  $1.65 \times 10^3$  to  $3.30 \times 10^5$ , the fluorescence peak at 525 nm increases from 57 counts to 378 counts (net counts). The same situation also applies to

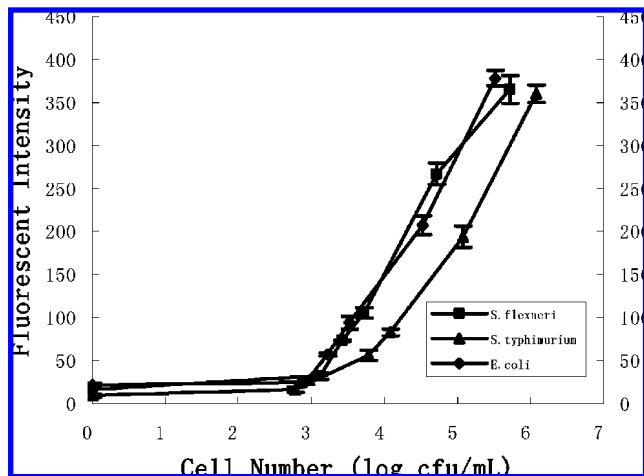


**Figure 9.** Intensities of fluorescence peaks at 625, 570, and 525 nm as produced by *S. typhimurium*, *S. flexneri*, and *E. coli* O157:H7 of the concentrations. Integration time, 512 ms; error bars =  $\pm$ SD ( $n = 3$ ).

*S. typhimurium* and *S. flexneri*. The counts of fluorescence peaks produced by *S. flexneri* and *S. typhimurium* increase by five times and four times, respectively, while the concentrations of bacterial cells increase 200 times. The background sample consisting of sterile water (no bacterial cells) still received 9–18 counts in the FI test (data not shown), which implies that there is nonspecific binding between magnetic beads and antibody-immobilized QDs. Another factor that may contribute to the inaccuracy in the assay is the cross-reactivity between bacterial cells and antibodies on the magnetic beads (17). In previous studies (22, 27, 28), however, it has been shown that the interaction between antibodies and bacterial cells was highly specific. Nonetheless, to eliminate the influence of these nonspecific signals, a criterion has been set in which a FI count lower than 20 would not be calculated and included in the statistic analysis. Despite the low level of nonspecific binding, these different tested bacterial cells have still produced highly selectable and specific fluorescence signals in the same assay.

**Figure 9** shows the FI at 525, 565, and 625 nm produced by reporter concentrations of *S. typhimurium*, *E. coli* O157:H7, and *S. flexneri* in the MSs. The FI counts increase substantially when the cell numbers increase from  $10^3$  to  $10^5$  cfu/mL. Interestingly, the increase of FI slowed down at higher concentrations of *S. flexneri* (from  $10^4$  to  $10^5$  cfu/mL), whereas the FI counts of *S. typhimurium* and *E. coli* O157:H7 still increase at the same slope. This may be due to the nonspecific binding and the saturation of specific antigen recognition. It is noted that the detection limits of this method for all three of the species are in the order of  $10^3$  cfu/mL by thresholding the signal level higher than the nonspecific signal ( $\sim 20$  counts). However, different species exhibit different sensitivities to the IMS-antibody-QDs detection method. Some species, such as *E. coli* O157:H7 and *S. flexneri*, are more sensitive to this method, and the detection limit is  $8.2 \times 10^2$  and  $1.3 \times 10^3$  cfu/mL, respectively, whereas for *S. typhimurium*, the cell numbers need to be  $6.0 \times 10^3$  cfu/mL to produce a detectable signal. Similarly, as shown in **Figure 9**, the signals produced by *E. coli* O157:H7 and *S. flexneri* have comparable intensities at the same cell concentration. However, the signals produced by *S. typhimurium* in the mixture are much lower than those at the same cell concentration of *E. coli* O157:H7 and *S. flexneri*. In a previous study (17), this phenomenon has been found in the detection of *E. coli* O157:H7 and *S. typhimurium* by the IMS-antibody-QDs method. It is suggested

**Table 2.** Results Obtained for the FI Counts of Bacteria Strains in Apple Juice and Milk

	food samples	dilution of samples	bacteria concentration in food samples	strain (wavelength)			
				<i>S. typhimurium</i> (625 nm)	<i>S. flexneri</i> (575 nm)	<i>E. coli</i> O157:H7 (525 nm)	<i>E. coli</i> DH5 $\alpha$ (525, 575, and 625 nm)
A	apple juice	10 <sup>-1</sup>	3.3 × 10 <sup>2</sup>	ND <sup>a</sup>	ND	ND	ND
		10 <sup>-1</sup>	3.3 × 10 <sup>3</sup>	ND	73 ± 5	72 ± 3	ND
		10 <sup>-1</sup>	3.3 × 10 <sup>4</sup>	52 ± 7 <sup>b</sup>	267 ± 21	180 ± 13	ND
		10 <sup>-1</sup>	3.3 × 10 <sup>5</sup>	152 ± 12	345 ± 31	312 ± 16	ND
		10 <sup>-1</sup>	3.3 × 10 <sup>5</sup> (MS)	160 ± 16	365 ± 23	345 ± 21	ND
	milk	10 <sup>-1</sup>	3.3 × 10 <sup>5</sup>	ND	ND	ND	ND
		10 <sup>-1</sup>	3.3 × 10 <sup>5</sup> (MS)	ND	ND	ND	ND
B	milk	10 <sup>-3</sup>	3.3 × 10 <sup>5</sup>	ND	ND	ND	ND
		10 <sup>-4</sup>	3.3 × 10 <sup>5</sup>	41 ± 3	245 ± 11	160 ± 15	ND
		10 <sup>-5</sup>	3.3 × 10 <sup>5</sup>	132 ± 9	325 ± 13	302 ± 22	ND
		10 <sup>-5</sup>	3.3 × 10 <sup>5</sup> (MS)	149 ± 14	348 ± 23	335 ± 19	ND
		10 <sup>-5</sup>	3.3 × 10 <sup>5</sup> (MS)				

<sup>a</sup> ND, not detected; net count ≤ 0. <sup>b</sup> The net peak of FI counts; data show the averages of five results.

that *S. typhimurium* has many serous types, which decreases the efficiency of recognition between antibody and cells when multicolonal antibodies are used in the detection.

**Result of Tests in Food Samples.** The feasibility of applying the method to the measurement of single species or mixed species food-borne bacteria in a complex concentration was studied. From the results shown in **Table 2**, we demonstrated that the FI counts increased rapidly with the increasing cell number in apple juice. The sample containing *E. coli* O157:H7 and *S. flexneri* presented distinguishable net peak intensities of 72 and 73 counts, respectively, with cell numbers at 10<sup>3</sup>, whereas in the sample only containing *E. coli* DH5 $\alpha$ , which was set as a negative control, no specific net peak was detected in any tested dilution levels. These results indicated that this method has high selectivity by using separated emission spectra.

It is interesting that bacteria in mixture samples obtained higher FI counts than in samples that only contained single strains. We believe that the most likely reason for this slight difference is due to the cross-reactions between nonspecific conjugation between QD-antibody and bacterial cells. However, at low concentration levels of bacterial cells, such as ×10 (data not shown), ×10<sup>2</sup>, and ×10<sup>3</sup> (such as *S. typhimurium*), it is difficult to detect specific emission peaks (~20 counts) in these samples. All sample matrixes in **Table 2** were positively detected by the China national standard of microbiological examination of food hygienic determination method when they were contaminated by *S. typhimurium*, *S. flexneri*, and *E. coli* O157:H7, respectively (data not shown).

In this study, milk was a complex matrix containing high levels of lipids, sugar, and proteins, which may have influenced the performance of the immunoassay. As shown in **Table 2**, no specific signal was counted even when the cell concentration was as high as ~10<sup>5</sup> when the sample was only diluted 10-fold. Only after the milk sample was diluted more than 1000-fold were specific counts detected in tested sample. Even in the detectable samples, the FI was much lower than the data collected from apple juice sample. Consistent with a previous report, when the fluorescence immunoassay was exploited in the detection of contaminants in milk samples, a strong baseline fluorescence signal significantly interfered with the detection (29). To solve this problem, these matrixes had to be simplified to obtain the necessary sensitivity. Some simplification methods that included a deproteinization procedure, however, might have removed bacterial cells at the same time. As a result, dilution and pre-enrichment of samples were utilized in this study. In this study, when milk sample was diluted ×10<sup>4</sup>, we were able to obtain specific signals of 160, 245, and 41 counts (*E. coli* O157:H7, *S. flexneri*, and *S. typhimurium*, respectively).

The ability to specifically and precisely detect multiple kinds of food-borne bacteria is in high demand. We have demonstrated a simple and rapid method for the simultaneous detection of *E. coli* O157:H7, *S. typhimurium*, and *S. flexneri* using fluoroimmunoassay. In this method, magnetic microbeads have been used for the efficient target capturing, and QDs have been used for the fluorescence labeling. We have been able to detect food-borne bacterial pathogens at the concentration of ~10<sup>3</sup> (*E. coli* O157:H7 and *S. flexneri*). Some pretreatment method of food samples needs to be developed to improve the detection limitation. This method can be used in the monitoring of several of the most important pathogens in different food matrixes simultaneously. Moreover, it provides the possibility to detect a panel of pathogens in food, agricultural, and environmental samples.

#### ACKNOWLEDGMENT

We thank Prof. Mingyuan Gao (Institute of Chemistry, Chinese Academic Association) for kindly providing the CdTe QDs and Prof. Qiangguo Chao (Shanghai Institute of Quality Inspection and Technical Research) for kindly providing bacterial strains.

#### LITERATURE CITED

- (1) Mead, P. S.; Slutsker, L.; Dietz, V.; McCaig, L. F.; Bresee, J. S.; Shapiro, C.; Griffin, P. M.; Tauxe, R. V. Food-related illness and death in the United States. *J. Environ. Health* **2000**, *62*, 9–18.
- (2) Wang, S.; Duan, H.; Zhang, W.; Li, J. W. Analysis of bacterial foodborne disease outbreaks in China between 1994 and 2005. *FEMS Immunol. Med. Microbiol.* **2007**, *51*, 8–13.
- (3) Rawool, D. B.; Malik, S. V. S.; Shakuntala, I.; Sahare, A. M.; Barbudhe, S. B. Detection of multiple virulence-associated genes in *Listeria monocytogenes* isolated from bovine mastitis cases. *Int. J. Food Microbiol.* **2007**, *113*, 201–207.
- (4) Wang, X. W.; Zhang, L.; Jin, L. Q.; Jin, M.; Shen, Z. Q.; An, S.; Chao, F. H.; Li, J. W. Development and application of an oligonucleotide microarray for the detection of food-borne bacterial pathogens. *Appl. Microbiol. Biotechnol.* **2007**, *76*, 225–233.
- (5) Hochel, I. Detection of *Campylobacter* species in foods by indirect competitive ELISA using hen and rabbit antibodies. *Food Agric. Immunol.* **2007**, *18*, 151–167.
- (6) Ochoa, M. L.; Harrington, P. B. Immunomagnetic isolation of enterohemorrhagic *Escherichia coli* O157: H7 from ground beef and identification by matrix-assisted laser desorption/ionization time-of-flight mass spectrometry and database searches. *Anal. Chem.* **2005**, *77*, 5258–67.
- (7) Su, X. L.; Li, Y. Quantum dot biolabeling coupled with immunomagnetic separation for detection of *Escherichia coli* O157: H7. *Anal. Chem.* **2004**, *76*, 4806–4810.

- (8) Shroyer, M. L.; Bhunia, A. K. Development of a rapid 1-h fluorescence-based cytotoxicity assay for *Listeria* species. *J. Microbiol. Methods* **2003**, *55*, 35–40.
- (9) Pyle, B. H.; Broadaway, S. C.; McFeters, G. A. Sensitive detection of *Escherichia coli* O 157: H 7 in food and water by immunomagnetic separation and solid-phase laser cytometry. *Appl. Environ. Microbiol.* **1999**, *65*, 1966–1972.
- (10) Dill, K.; Stanker, L. H.; Young, C. R. Detection of *salmonella* in poultry using a silicon chip-based biosensor. *J. Biochem. Biophys. Methods* **1999**, *41*, 61–67.
- (11) Islam, M. S.; Hossain, M. Z.; Khan, S. I.; Felsenstein, A.; Sack, R. B.; Albert, M. J. Detection of non-culturable *Shigella* dysenteriae 1 from artificially contaminated volunteers' fingers using fluorescent antibody and PCR techniques. *J. Diarrhoeal Dis. Res.* **1997**, *15*, 65–70.
- (12) Agrawal, A.; Sathe, T.; Nie, S. Single-bead immunoassays using magnetic microparticles and spectral-shifting quantum dots. *J. Agric. Food Chem.* **2007**, *55*, 3778–3782.
- (13) Jaiswal, J. K.; Mattoussi, H.; Mauro, J. M.; Simon, S. M. Long-term multiple color imaging of live cells using quantum dot bioconjugates. *Nat. Biotechnol.* **2003**, *21*, 47–51.
- (14) Bhunia, A. K.; Banada, P.; Banerjee, P.; Valadez, A.; Hirtleman, E. D. Light scattering, fiber optic-and cell-based sensors for sensitive detection of foodborne pathogens. *J. Rapid Methods Autom. Microbiol.* **2007**, *15*, 121–145.
- (15) Hahn, M. A.; Tabb, J. S.; Krauss, T. D. Detection of single bacterial pathogens with semiconductor quantum dots. *Anal. Chem.* **2005**, *77*, 4861–4869.
- (16) Zhu, L.; Ang, S.; Liu, W. T. Quantum dots as a novel immunofluorescent detection system for *Cryptosporidium parvum* and *Giardia lamblia*. *Appl. Environ. Microbiol.* **2004**, *70*, 597–578.
- (17) Yang, L.; Li, Y. Simultaneous detection of *Escherichia coli* O157: H7 and *Salmonella typhimurium* using quantum dots as fluorescence labels. *Analyst* **2006**, *131*, 394–401.
- (18) Chen, W.; Shen, H.; Li, X.; Jia, N.; Xu, J. Synthesis of immunomagnetic nanoparticles and their application in the separation and purification of CD<sup>34+</sup> hematopoietic stem cells. *Appl. Surf. Sci.* **2006**, *253*, 1762–1769.
- (19) Yang, H. H.; Zhang, S. Q.; Chen, X. L.; Zhuang, Z. X.; Xu, J. G.; Wang, X. R. Magnetite-containing spherical silica nanoparticles for biocatalysis and bioseparations. *Anal. Chem.* **2004**, *76*, 1316–1321.
- (20) Xing, Y.; Chaudry, Q.; Shen, C.; Kong, K. Y.; Zhou, H. E.; Chung, L. W.; Petros, J. A.; Mo'Regan, R.; Yezhelyev, M. V.; Simons, J. W. Bioconjugated quantum dots for multiplexed and quantitative immunohistochemistry. *Nat. Protoc.* **2007**, *2*, 1152–1165.
- (21) Hua, X. F.; Liu, T. C.; Cao, Y. C.; Liu, B.; Wang, H. Q.; Wang, J. H.; Huang, Z. L.; Zhao, Y. D. Characterization of the coupling of quantum dots and immunoglobulin antibodies. *Anal. Bioanal. Chem.* **2006**, *386*, 1665–1671.
- (22) Clapp, A. R.; Goldman, E. R.; Mattoussi, H. Capping of CdSe-ZnS quantum dots with DHLA and subsequent conjugation with proteins. *Nat. Protoc.* **2006**, *1*, 1258–1266.
- (23) Hu, F.; Ran, Y.; Zhou, Z.; Gao, M. Preparation of bioconjugates of CdTe nanocrystals for cancer marker detection. *Nanotechnology* **2006**, *17*, 2972–2977.
- (24) Clapp, A. R.; Medintz, I. L.; Uyeda, H. T.; Fisher, B. R.; Goldman, E. R.; Bawendi, M. G.; Mattoussi, H. Quantum dot-based multiplexed fluorescence resonance energy transfer. *J. Am. Chem. Soc.* **2005**, *127*, 18212–18221.
- (25) Goldman, E. R.; Clapp, A. R.; Anderson, G. P.; Uyeda, H. T.; Mauro, J. M.; Medintz, I. L.; Mattoussi, H. Multiplexed toxin analysis using four colors of quantum dot fluororeagents. *Anal. Chem.* **2004**, *76*, 684–688.
- (26) Szab, D. V.; Vollath, D. Nanocomposites from coated nanoparticles. *Adv. Mater.* **1999**, *11*, 1313–1313.
- (27) Yang, L.; Li, Y. Quantum dots as fluorescent labels for quantitative detection of *Salmonella typhimurium* in chicken carcass wash water. *J. Food Prot.* **2005**, *68*, 1241–1245.
- (28) Islam, D.; Tzipori, S.; Islam, M.; Lindberg, A. A. Rapid detection of *Shigella dysenteriae* and *Shigella flexneri* in faeces by an immunomagnetic assay with monoclonal antibodies. *Eur. J. Clin. Microbiol. Infect. Dis.* **1993**, *12*, 25–32.
- (29) Luo, L.; Zhang, Z.; Chen, L.; Ma, L. Chemiluminescent imaging detection of staphylococcal enterotoxin C1 in milk and water samples. *Food Chem.* **2006**, *97*, 355–360.

---

Received for review September 14, 2008. Revised manuscript received November 19, 2008. Accepted November 20, 2008. This work was supported by the National Nature Science Foundation of China (20573075, 20773088), the National Basic Research Program of China (2008CB617504), the Shanghai Science and Technology Committee (06DZ05137, 0752nm028), and the Shanghai Key Laboratory of Rare-earth Functional Materials (07dz22303).

JF802817Y